Energy 254 (2022) 124357

Contents lists available at ScienceDirect

Energy

journal homepage: www.elsevier.com/locate/energy

Analysis of energy demand in a residential building using TRNSYS

Magdi Rashad [a], Alina Żabnieńska-Góra [a, b], Les Norman [a], Hussam Jouhara [a, c, *]

[a] Heat Pipe and Thermal Management Research Group, College of Engineering, Design and Physical Sciences, Brunel University London, UB8 3PH, UK
[b] Wroclaw University of Science and Technology, Faculty of Environmental Engineering, Wybrzeze Wyspianskiego 27, 50-370, Wroclaw, Poland
[c] Vytautas Magnus University, Studentu Str. 11, LT-53362, Akademija, Kaunas Distr., Lithuania

ARTICLE INFO

Article history:
Received 21 February 2022
Received in revised form
17 May 2022
Accepted 21 May 2022
Available online 25 May 2022

Keywords:
Energy demand
Building model
GoogleSketchU
Plug-in
PMV
PPD
TRNSYS simulation

ABSTRACT

Energy simulations of buildings complement or replace the static calculations used so far and provide detailed answers to questions such as: what is the energy demand for individual purposes in a building and how does it change over the course of a day, a month, a year and also enable a comparison of several design variants and the selection of the optimal one in terms of energy consumption. Therefore, energy simulations of buildings help make decisions to optimise architectural and installation solutions, leading to a reduction in electricity, gas and water demand for the designed building. They indicate to what extent individual factors affect the demand for heating, cooling and electricity. The results of the analyses can be used as a basis for design and system decisions, and also provide interesting feedback to the investor.

This paper focuses on the year-round analysis of a three-zone building in TRNSYS. Attention is given to the values of the heat transfer coefficients through the envelope, heating and cooling demand, the effect of heat gains/losses on the energy demand of the building and thermal comfort. The article points out that the correct determination of the energy needs of a building influences the correct choice of renewable energy source and the lowest cost of installation.

1. Introduction

The demand for electricity is high and is increasing year by year. At the same time its production still relies heavily on fossil fuels, which has a negative impact on the environment.

The increase in greenhouse gas production has prompted the world community to set ambitious targets to prevent global warming [1–4]. In the third quarter of 2021 total UK total energy production was 25.1 million tonnes of oil equivalent [5]. Compared to the third quarter of 2020, total final energy consumption was 6.4% higher. It is significant that the share of renewable energy sources in electricity generation is increasing, as can be seen in Fig. 1. The temporary decline in summer 2021 was due to maintenance work on the North Sea limiting renewable energy production as well as lower wind speeds. The share of photovoltaic (PV) systems recorded an increase to 6.2% in 2021, as illustrated in Fig. 2.

In the UK, the domestic electricity consumption is one of the largest consumers [5] thus solar PV systems for residential users are among the most preferred installations. PV systems allow electricity to be generated from 100% renewable solar energy [6]. The energy obtained can be used for the operation of household appliances, and/or for heating and domestic hot water [7]. Over the last 20 years, there has been a significant increase in the number of PV installations [8]. Ahmad L. et all [9]. extensively discussed the latest technological developments in the different types of solar collectors. UK Solar deployment by capacity and accreditation is shown in Fig. 3. According to the data presented, there is a total of 13,654 MW of installed solar capacity in the UK sited at 1,121,819 installations at the end of December 2021 [8].

The cost of the installation is a key issue for the individual consumer. Since 2013, detailed costs for small installations in the 0–4 kW, 4–10 kW and 10–50 kW ranges from the Microgeneration Certificate Scheme (MSC) have been posted on government websites [10] The MCS Installations Database contains information on certified small scale, low carbon installation in the UK since 2010 [11]. It should be noted that the data available [10] does not represent the cost to the householder. It is the cost per kW resulting from dividing the total cost (which include the cost of the photovoltaic generation equipment, the cost of installation and

* Corresponding author. Heat Pipe and Thermal Management Research Group, College of Engineering, Design and Physical Sciences, Brunel University London, UB8 3PH, UK.

E-mail address: hussam.jouhara@brunel.ac.uk (H. Jouhara).

https://doi.org/10.1016/j.energy.2022.124357

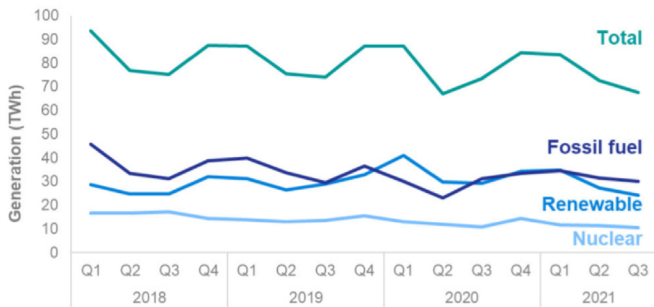

Fig. 1. Electricity generated, by fuel type in UK [5].

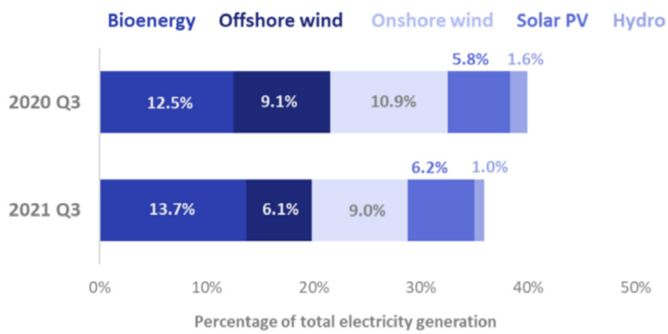

Fig. 2. Renewables' share of electricity generation – Q3 2020 and Q3 2021 [5].

connection to the electricity grid and VAT) by the installed capacity. 28,638 installations were included in the analysis between April 2019 and March 2020. According to the statistics, the average cost of solar PV installations in 2020/21, despite an increase on the previous year 2019/2020, for 0–4 kW installations was 10% lower than in 2018/19 and 28% lower than in 2013/14 and was £1628 per kW installed. The average cost of a 4–10 kW installation was £1685 per kW installed in 2021/2022 and for 10–50 kW £1088.

Currently, photovoltaic systems can be grid-connected (On-grid) or stand-alone (Off-grid) [12]. However, the cost of the installation is significantly influenced by the building structure, its location and occupancy [13]. In order to select a PV system, it is necessary to find out what the annual energy demand of the building will be. Energy simulation programs that take these factors into account can help to find the most energy-optimal building design and thus contribute to minimizing the PV installation costs.

This article focuses on the building and the factors that have the greatest impact on energy demand. Therefore, a step-by-step construction of the building model in TRNSYS is presented. The phase of defining building geometry, wall structures, heating and cooling loads, infiltration, gains and schedules is described in detail. For each of these stages, the energy demand was investigated. In addition, the PMV and PPD values for the analysed building were examined.

2. Building energy simulation

Modelling the behaviour of a building under changing operating conditions enables detailed analyses to be carried out, which will contribute to key decisions being made both at the stage of designing a building and retrofitting an existing one. The energy simulations software's provide the ability to predict the performance of the designed building, the selected systems or both at the same time. They allow for a more complete description of those phenomena that cannot be characterised by simple static calculations such as the way a building reacts to solar heat gains or the accumulation in partitions.

There are a number of software packages that can analyse either buildings, systems or both at the same time such as TRNSYS, EnergyPlus or IDA ICE. Each has its advantages and limitations. Each of these has been described many times in the literature [14–17].

In addition, M. Magni et al. [18] compared them with respect to modelling approaches and computational costs. The authors highlighted that it required many iterations to achieve good agreement in the representation of the building across the different programs. To assess compliance, statistical indicators were used among others. A. Chong et all [19]. addressed the issue of model calibration to improve the reliability of simulations. The article provides definitions of calibration, validation and verification according to the American Institute of Aeronautics and Astronautics (AIAA) guide and the article by T.G. Trucano et al. [20].

TRNSYS software allows the simulation of different types of solar collector, photovoltaics as well as photovoltaic-thermal (PV/T) collector [21,22], heat pipe heat exchangers [23,24], PVT-collector model and horizontal ground heat exchanger [25], solar-assisted ground-source heat pumps [26] as well as the building [27] or

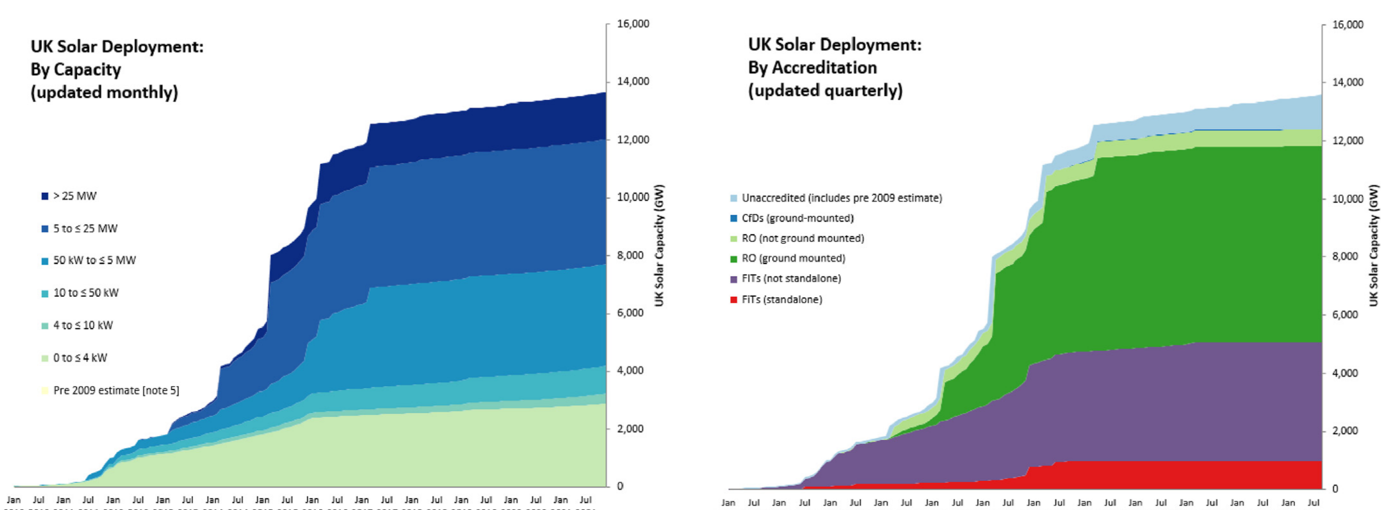

Fig. 3. UK Solar deployment by capacity and accreditation [8].

multiple radiative inter-reflections exchanges [28]. Both the system and the building can be configured and analysed separately.

Researchers are interested in the potential of waste heat recovery in residential buildings [29], reducing the risk of disease transmission by analysing ventilation strategies [30] or using useful ambient energy [31]. However, a basic analysis of the energy needs of the building itself to maintain thermal comfort has not been widely investigated.

After reviewing the various functionalities of each package, TRNSYS was selected for the building analysis. This article focuses on the building and the factors that have the greatest impact on energy demand. TRNSYS enables multi-zone building modelling with Type56 and TRNBuild. The user can map the thermal behaviour of a building divided into different zones and then assign heating, cooling, humidification, operating schedules, gains and much more to the model.

2.1. Building geometry

The modelling process begins by defining the geometry. The more complex the shape, the more difficult it is to represent it in the programme. For this purpose, the Trnsys3d plug-in for Google Sketchup may be used. This solution allows the elements of self-shading of the building to be taken into account or for radiation exchange internal view factors [32]. Correct definition of individual zones, windows, external and internal partitions in SketchUp speeds up the design process, and due to the visualisation the whole process is user-friendly. The generated file with a.IDF (Indermeidate Data File) extention can be imported into TRNSYS by creating a new 3D project (multizone). At this stage the following can be assigned: weather data file, building orientation, boundary temperatures of surfaces, static distribution factor of solar direct radiation or shading control. To modify a building in the TRNSYS project window, the building needs to be edited in TRNBuild.

For the purposes of this article, a three-zone building was prepared in Google Sketchup and then imported into TRNSYS according to the above guidelines (Fig. 4A). The implemented geometry can be seen in TrnViewBUI as shown in Fig. 4B. In order to calculate the correct azimuthal angles of the surface orientation, the northern hemisphere was defined. London weather data has been assigned. The building is divided into three zones: on the ground floor North (SunZone) and South (BackZone) zones with a surface area of 20 m^2 each. Above them there is an unheated attic of 40 m^2. 2.4 m^2 of windows have been placed in the northern and southern walls.

2.2. Heat transfer coefficient

For the next stage of the building modelling process, an appropriate structure must be assigned to the individual building envelopes, taking into account the heat transfer coefficient U. This is one of the most important steps as it determines the amount of energy that needs to be supplied to the building in order to maintain the air temperature in each zone at the desired level. Maintaining thermal comfort indoors is crucial. Thermal comfort depends on the indoor air temperature and the surface temperature of the building envelope (preferably a difference of less than 3 K) as well as air speed (above 0.15 m/s giving sensations of draught) and humidity (the comfort range is 40–70%). Suitable insulation slows down the flow of heat through surfaces such as walls, attic and roof. The house stays warm in winter and at the same time in summer the insulation will keep the building pleasantly cool.

Optimisation efforts start with the choice of envelope materials, glazing type or the entire façade, as these factors have a fundamental impact on the energy efficiency of the building [33–35]. Using simulation tools, the energy requirements for any configuration can be predicted. Every building, whether newly constructed, sold or rented out, should have an Energy Performance Certificate (EPC) indicating the energy efficiency of the building. Energy efficiency refers to the cost of the fuel that has to be supplied and the carbon dioxide emissions. The scores associated with each energy efficiency band are as follows [36]: band A – 92 plus (most efficient); band B – 81 to 91; band C – 69 to 80; band D – 55 to 68; band E – 39 to 54; band F – 21 to 38; band G – 1 to 20 (least efficient).

According to Office for National Statistic [36], by March 2021 the median energy efficiency score for residential dwellings in England was 66 which corresponds to band D. Median energy efficiency score by tenure and property type in England is shown in Fig. 5.

In the simplified calculation method U value according to the standard [38] is described as:

$$U = \frac{1}{R_{tot}} \tag{1}$$

where: U, R_{tot} is the thermal transmittance (W/(m^2K)) and the total thermal resistance (m^2K/W) respectively. The total thermal resistance of a flat building element for which the heat flow is perpendicular to the stacked, thermally homogeneous layers can be defined as:

$$R_{tot} = R_{si} + R_1 + R_2 + R_n + R_{se} \tag{2}$$

where R_{tot}, R_{si}, R_{se} is the total thermal resistance (m^2K/W), the internal surface resistance (m^2K/W) and the external surface resistance (m^2K/W) respectively. R_1; R_2,R_n are the design thermal resistances of each layer (m^2K/W); The thermal resistance of the layer can be described as a function of thermal conductivity (W/(mK)) and material layer thickness d (m):

$$R = \frac{d}{\lambda} \tag{3}$$

For the purposes of this article, the requirements for external walls in terms of heat transfer coefficient for wall, floor, window and roof construction have been assigned as follows: external wall 0.16 W/(m^2K), floor 0.11 W/(m^2K), roof 0.11 W/(m^2K), window 1.1 W/(m^2K). The order of layers is precisely defined. For each wall construction material used the following is given: layer thickness [m], thermal conductivity [kJ/h m K], specific heat capacity [kJ/kg K] and density [kg/m^3]. Each wall can consist of up to 20 layers. In addition, for each partition it is possible to specify solar absorptance, longwave emission coefficient, convective heat transfer coefficient for both sides of the walls: front and back. In TRNSYS both the front and back of every wall are assumed to be black for internal radiative gains and for long-wave radiation exchange between the internal surfaces [39]. Type 56 also gives the option of defining to a specific wall area a specific energy flux.

The results of the simulation with the defined partition structure taking into account the variation of ambient, ground, air and operative temperature in each zone are illustrated in Fig. 6.

The results clearly show that the lack of a heat source, when appropriate values of heat transfer coefficients for London are used, does not allow the room temperature to be maintained at 20 °C in any of the zones. The variation of the internal temperature follows the ambient temperature. Maintaining the required temperature in a room requires the supply of heat. The amount of heat to be supplied to each zone is precisely defined and independent of the type of heat source.

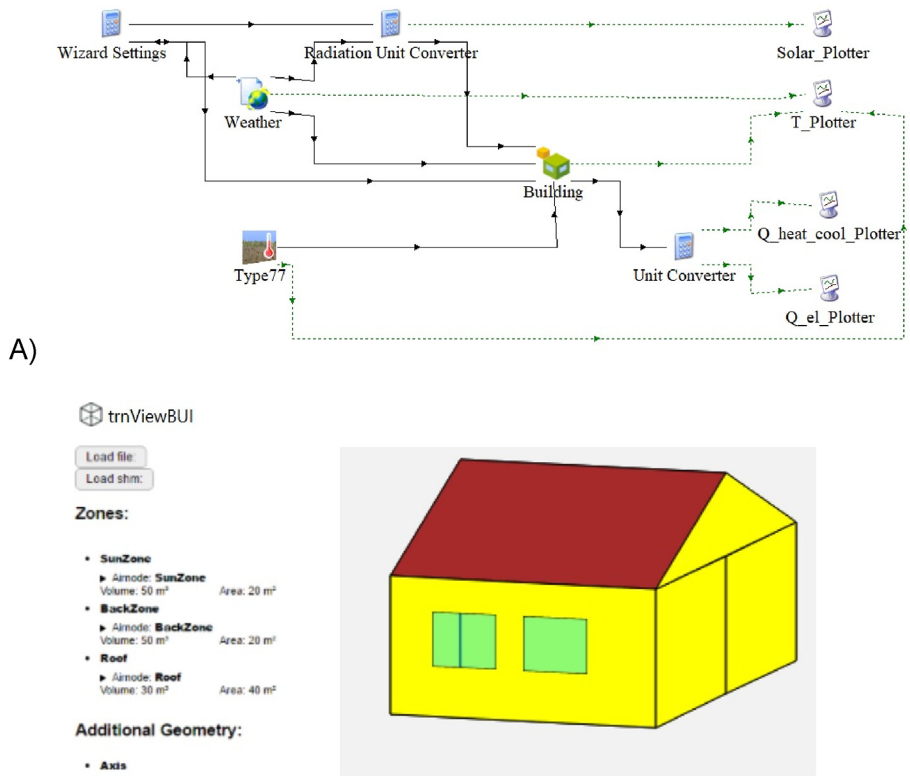

Fig. 4. View of A)Simulation Studio: TRNSYS project b)TRNBuild: 3 zone building in trnViewBUI.

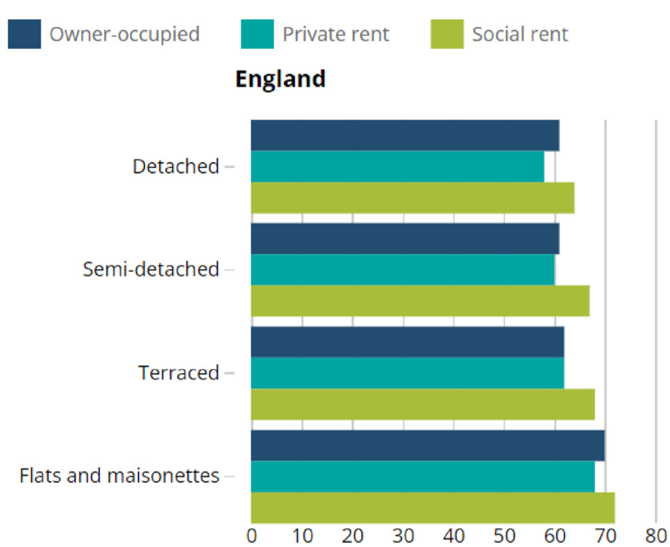

Fig. 5. Median energy efficiency score by tenure and property type in England [36]. Maintaining proper thermal and humidity conditions will be achieved by meeting the legal requirements for the energy performance of the building. In England the current standard is: The Building Regulations 2010 Conservation of fuel and power APPROVED DOCUMENT L Volume 1: Dwellings 2021 edition – for use in England [37]. Limiting U-values are presented in Table 1.

2.3. Heating and cooling load

The default setting for the heating and cooling control in TYPE56 is OFF. This means that in order to determine the energy required for heating or cooling in each zone the ideal control option must be activated. However, it must be remembered that in this situation the heating and cooling devices are not modelled outside the TYPE56 component. Otherwise this function should not be used. In heating mode, the room setpoint temperature, the heating power with its radiative part, and the humidification of the air within the air-node can be determined.

In cooling mode, the room setpoint temperature, cooling capacity and zone dehumidification can be specified. All variables can be defined as a constant, an input, or a schedule. Schedules are periodic functions [39]. Depending on the time of day and/or week, the output may change. In addition, TRNSYS allows the user to simulate heating devices that provide part of their power through convection and part via radiation. At these settings, a defined fraction of the radiating power of the heater is supplied as internal radiation gains and distributed to the walls of the zone. The software allows surface heating to be modelled, but this must be taken into account when defining floor, wall or ceiling constructions.

For this article, the constant temperature is set to 20 °C degrees in winter and 25 °C degrees in summer. In more detailed simulations, the heating can be set according to a schedule, for example, the room temperature can be reduced at night. Figs. 7 and 8 show the simulation results for a building with unlimited heating and cooling. The Fig. 8 indicates that the northern zone does not reach the minimum temperature of 25 °C in summer when the cooling system has to be activated. The cooling demand in the southern zone, where solar gains are higher than in the northern zone, is a maximum of 13.6 W/m^2. According to the simulation, the heat demand does not exceed 9.24 W/m^2 floor area. By using the TYPE 65c component in Simulation Studio, which allows data to be printed to a file, the exact values of the heating and cooling demand were investigated.

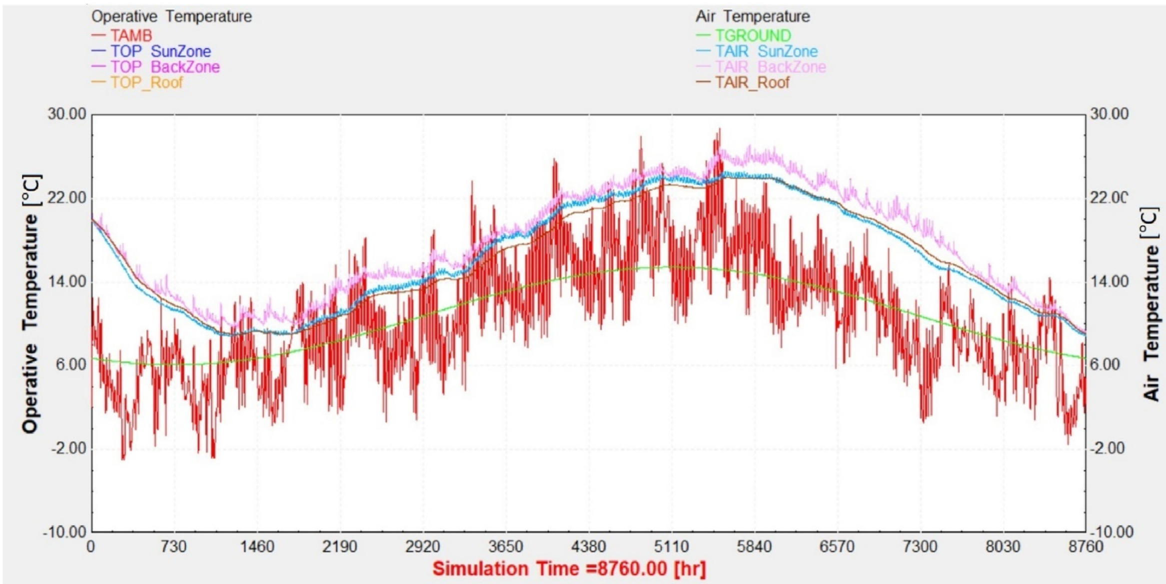

Fig. 6. The variability in ambient, ground, operative and air temperature in each zone.

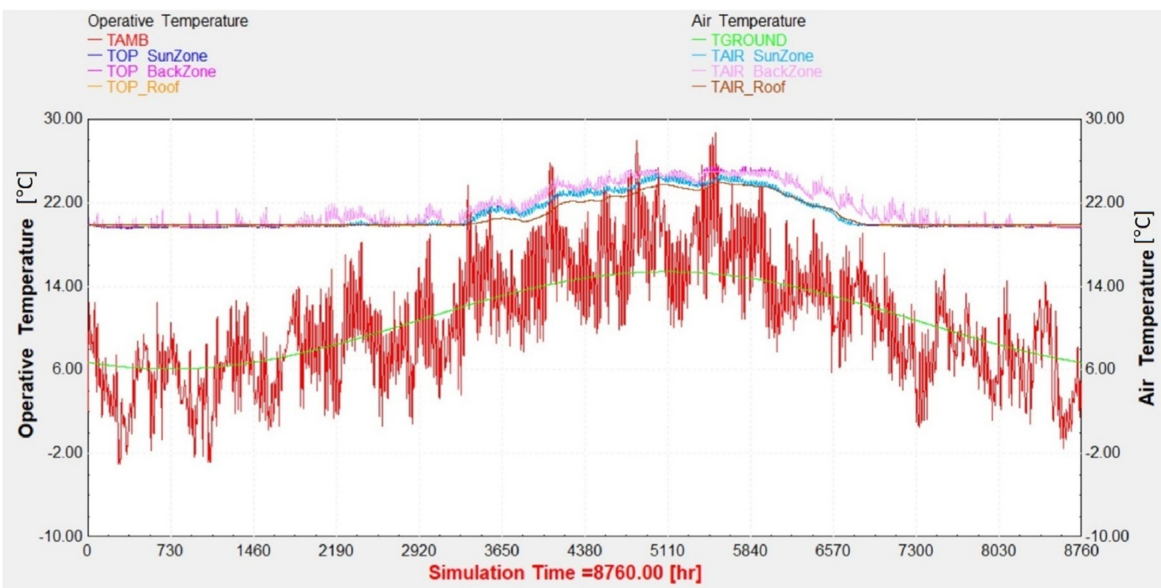

Fig. 7. The variability in ambient, ground, operative and air temperature in each zone with defined space heating and cooling.

2.4. Infiltration, gains and schedules

For a house, the total steady state design heat loss coefficient is determined by the sum of fabric (envelop) losses, infiltration and any ventilation loss, and is calculated in accordance with Heating CIBSE Guide B1: 2016 [40]. According to the guidelines, infiltration (Air infiltration allowance air changes/h) for houses depends on the type of room and should be adequate with the following values: living rooms 1, bedrooms 0.5, bathrooms 2, staircases and corridors 1.5.

Steady state heat loss due to infiltration is described by the following formulae:

$$\Phi_{inf} = q_{inf}\rho c_p(\theta_{ai} - \theta_{ao}) \tag{4}$$

where q_{inf} is the infiltration rate (m^3/s), ρ is the air density (kg/m^3), c_p is the specific heat capacity of air at constant pressure (J/kg·K), θ_{ai} and θ_{ao} is the inside and outside air temperature (°C).

Steady state ventilation heat loss is given by the:

$$\Phi_v = q_v\rho c_p(\theta_{ai} - \theta_{vs}) \tag{5}$$

where q_v is the ventilation rate (m^3/s) and θ_{vs} is the temperature at which the air enters the room (°C).

The standard approach neglects any heat gains in the room that result from occupants, lighting and equipment. For rooms that are permanently occupied and used this is inappropriate.

TRNBuild allows all these factors to be taken into account for the building under consideration and much more. As an example, the energy balance for zones (NTYPE 904) is described below [39]:

$$Q_{BAL} = -DQ_{AIRdt} + Q_{HEAT} - Q_{COOL} + Q_{INF} + Q_{VENT} + Q_{COUP} + Q_{TRANS} + Q_{GINT} + Q_{WGAIN} + Q_{SOL} + Q_{SOLAIR}\ [kJ/hr] \tag{6}$$

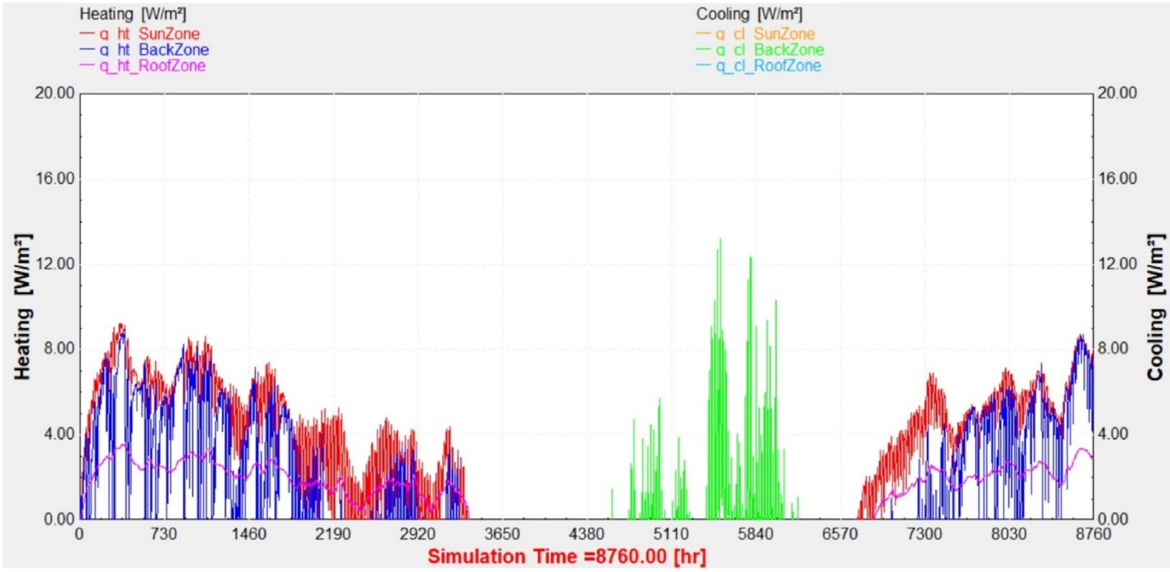

Fig. 8. Heating and cooling demand in each zone.

Where:

DQ_{AIRdt} - change of internal energy of zone (calculated with capacitance of air + additional capacitance which might be added in TRNBuild)
Q_{HEAT} - power of ideal heating (convective + radiative)
Q_{COOL}-power of ideal cooling
Q_{INF}- infiltration gains
Q_{VENT} - ventilation gains
Q_{COUP} - coupling gains
Q_{TRANS} - transmission into the surface from inner surface node (might be stored in the wall, going to a slab cooling or directly transmitted)
Q_{GINT} - internal gains (convective + radiative)
Q_{WGAIN} - wall gains
Q_{SOL} - absorbed solar gains on all inside surfaces of zones
Q_{SOLAIR} - convective energy gain of zone due transmitted solar radiation through external windows which is transformed immediately into a convective heat flow to internal air.

For the concerned building, internal gains (including persons), electrical equipment and lighting, have been defined on the basis of a very extensive library which, for example, allows the determination of internal gains based on ASHRAE guidelines, EN13779, VDI2078 or SIA 2024. In addition, a separate time schedule has been assigned for each of the gains. It is assumed that the residents work between 9 a.m. and 5 p.m. and therefore use the lighting between 6 a.m. and 8 p.m. and 6 p.m. and 11 p.m.

At weekends the household spend most of their time at home, leading a mostly sedentary lifestyle (according to ASHRAE Degree of Activity III — seated, very light work). No thermal comfort analysis was included in the considered building configuration. However, the software does allow for thermal comfort calculations

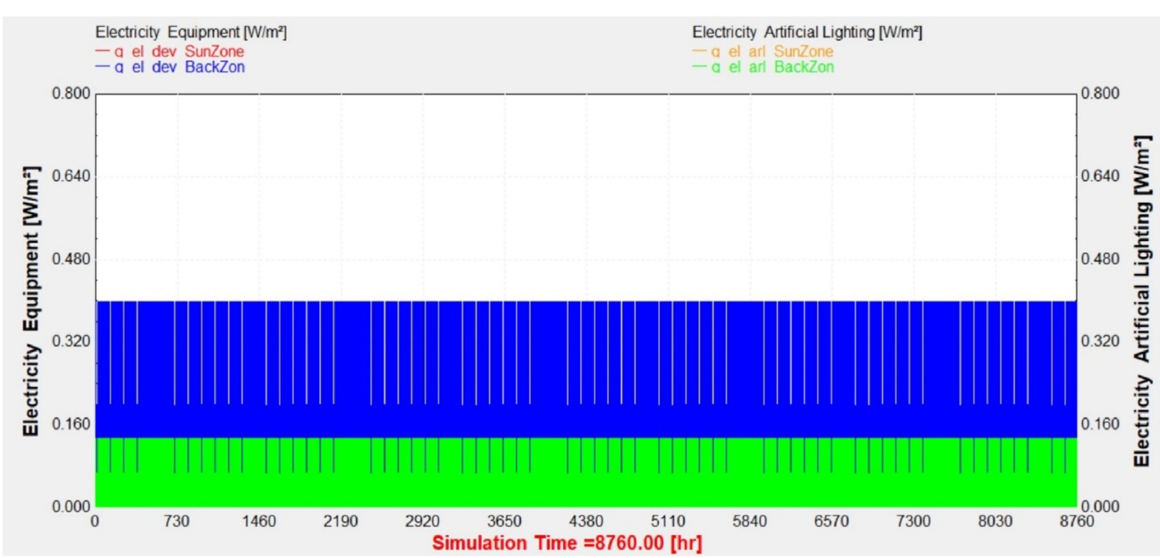

Fig. 9. Electricity demand in both zones.

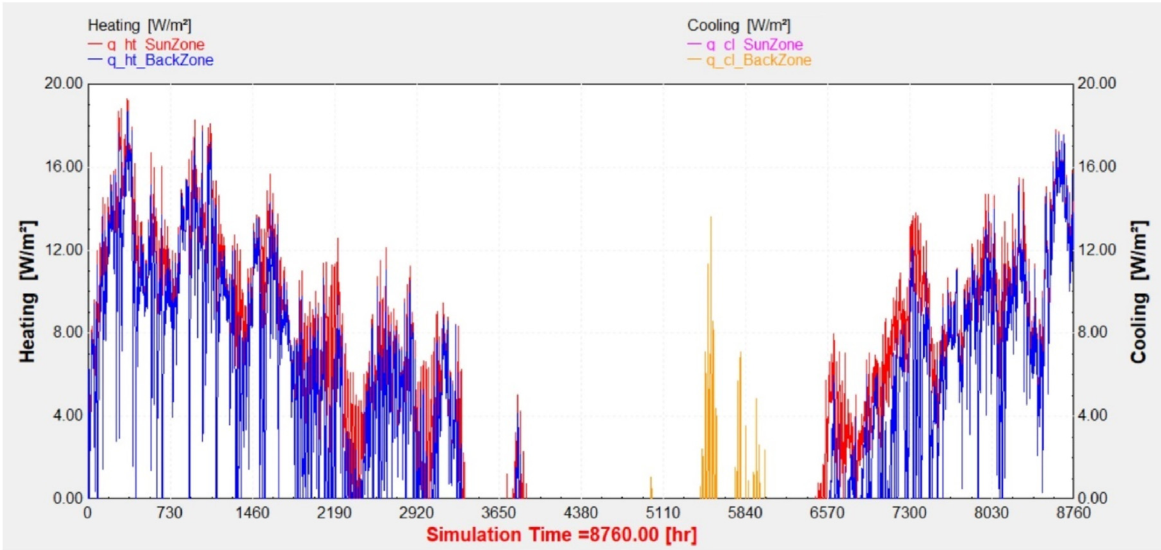

Fig. 10. Heating and cooling demand in each zone including internal gains and infiltration 0.6.

based on EN ISO 7730. Electricity demand is the same in both zones. Its level is shown in Fig. 9. For lighting is 0.135 W/m^2, for domestic appliances 0.4 W/m^2. Fig. 10 illustrates the heating and cooling demand taking into account the above-mentioned factors. In the next step of the analysis, it was investigated how the heat demand of a building would change when an infiltration of 0.6 AC/H (Air Change per Hour) was assigned in the model and then increased to 1. The results of the analysis carried out are presented in Fig. 11.

As can be seen from Figs. 10 and 11 the amount of heat delivered to the rooms increases significantly as the infiltration rate increases.

2.5. Thermal COMFORT

The final step of the analysis focused on thermal comfort. Thermal comfort is a state of heat balance in which a person is neither too cold nor too hot [41]. The main factors that influence the feeling of thermal comfort are: air temperature, air velocity, radiant temperature, relative humidity as well as clothing, metabolic heat or level of activity, wellbeing and occupant health status. Thermal comfort is a subjective feeling and therefore a standard had to be created to which one can refer. Two thermal comfort indices based on EN ISO 7730 [20] are commonly used: the predicted mean vote (PMV) and the predicted percentage dissatisfied (PPD). PPD determines the estimated number of people who are dissatisfied with the thermal conditions and can be determined from the following formula [42]:

$$PPD = 100 - 95 \times \left(-0.03353 \times PMV^4 - 0.2179 \times PMV^2 \right) \quad (7)$$

PMV is an index which determines the average value of the votes of a group of users on a seven-point scale of thermal sensations (Table 2). According to the standard [43], it may be determined as follows:

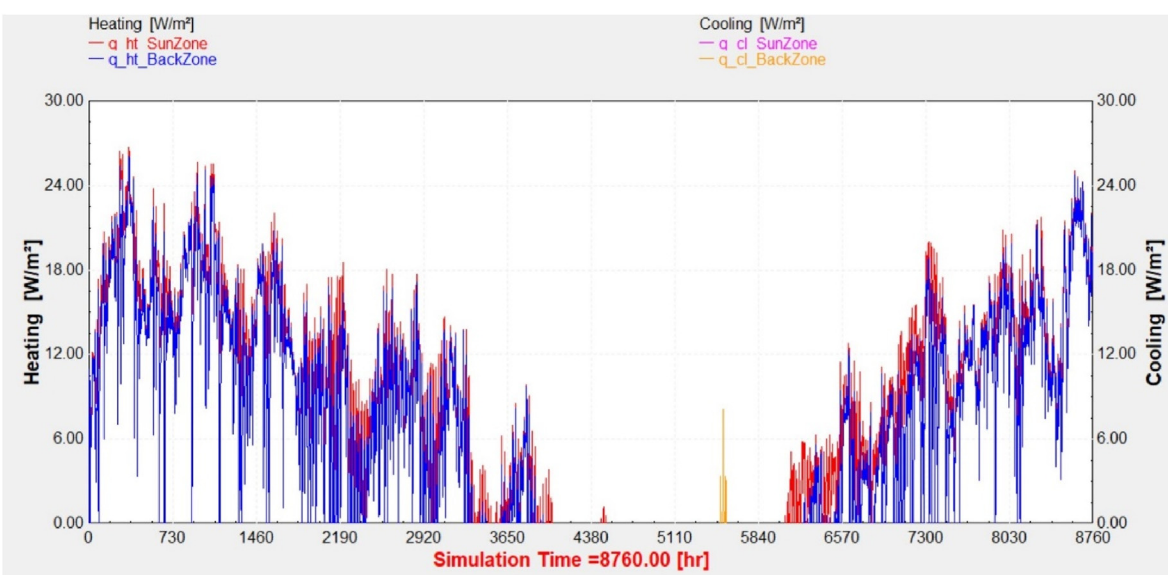

Fig. 11. Heating and cooling demand in each zone including internal gains and infiltration 1.

Table 1
Limiting U-values according to Ref. [37].

Element type	Limiting U-values for new fabric elements and air permeability in new dwellings	Limiting U-values for new fabric elements in existing dwellings	Limiting U-values for existing elements in existing dwellings (Improved)
	Maximum U-value W/(m²·K)	Maximum U-value W/(m²·K)	Maximum U-value W/(m²·K)
All roof types	0.16	0.15	0.16
Wall	0.26	0.18	Wall – cavity insulation: 0.55 Wall – internal or external insulation 0.3
Floor	0.18	0.18	0.25
Party wall	0.20		
Window	1.6	1.4 or Window Energy Rating Band B minimum	–
Rooflight	2.2	–	–
Doors (including glazed doors)	1.6	Doors with >60% of internal face glazed: 1.4 or Door-set Energy Rating Band C minimum Other doors: 1.4 or Door-set Energy Rating Band B minimum	–
Air permeability	8.0m³/(h·m²) @ 50Pa 1.57m³/(h·m²) @ 4Pa		

$$PMV = \left(0.303e^{-0.036M} + 0.028\right) \times \Big\{(M-W) - 3.05\times10^{-3} \times [5733 - 6.99(M-W) - P_a] - 0.42 \times (M-W) - 58.15\Big] - 1.7\times10^{-5}M(5867 - P_a) - 0.0014M(34 - t_a) - 3.96\times10^{-8}f_{cl} \times \left[(t_{cl}+273)^4 - (\overline{t_r}+273)^4\right] - f_{cl}h_c(t_{cl}-t_a)\Big\} \quad (8)$$

Where:

$$t_{cl} = 35.7 - 0.028(M-W) - I_{cl}\Big\{3.96\times10^{-8}f_{cl} \times \left[(t_{cl}+273)^4 - (\overline{t_r}+273)^4\right] - f_{cl}h_c(t_{cl}-t_a)\Big\} \quad (9)$$

$$h_c = \begin{cases} 2.38(t_{cl}-t_a)^{0.25} \; for \; 2.38\times|t_{cl}-t_a|^{0.25} > 12.1\sqrt{V_{ar}} \\ 12.1\sqrt{V_{ar}} \quad for \; 2.38\times|t_{cl}-t_a|^{0.25} < 12.1\sqrt{V_{ar}} \end{cases} \quad (10)$$

$$f_{cl} = \begin{cases} 1.00 + 1.290I_{cl} \; for \; I_{cl} \le 0.078m^2K/W \\ 1.05 + 0.645I_{cl} \; for \; I_{cl} > 0.078m^2K/W \end{cases} \quad (11)$$

where:

M is the metabolic rate [W/m²]
W is the effective mechanical power [W/m²] equal to zero for most activities
I_{cl} is the thermal resistance of clothing, [m² K/W]
f_{cl} is the ratio of surface area of the body with clothes to the surface area of the body without clothes
t_a is the air temperature, [°C]
t_r is the mean radiant temperature, [°C]
V_{ar} is the relative air velocity, [m/s]
P_a is the water vapor partial pressure, [Pa]
h_c is the convective heat transfer coefficient, [W/m²°C]
t_{cl} is the clothing surface temperature, [°C]

Based on EN ISO 7730 [20], the values for the building under consideration were assumed:

- the clothing factor of 0.6 was chosen: Light working ensemble (Athletic shorts, woollen socks, cotton work shirt, work trousers).
- metabolic rate: 1.2 seated, light work (office, home, school, laboratory).
- external work: 0
- relative air velocity: 1

An internal calculation - simple model was selected in which the calculation is based on an area weighted mean surface temperature of all surfaces of a zone [39]. Moreover, the calculation of PMV and PPD does not take into account the effects of diffuse or direct solar radiation on room occupants. In the developed model, in order to verify the PMV and PPD values, additional outputs were defined for TYPE56. The variability of PMV and PPD over the year is shown in Fig. 12. The results of the conducted simulations are summarized in Table 3. As can be seen, there is no difference in the amount of power needed to heat the rooms after the implementation of the heat comfort module.

However, at the same time, Fig. 12 indicates that the indoor conditions in the analysed rooms are not within the expected range of − 0.5 to + 0.5 for comfortable (ideal) conditions. Hence, the percentage of people dissatisfied (PPD) in the least favourable period of time is 15.2% and 15.14% for the Sun-Zone and Back-Zone, respectively. PMV values range from −0.7 to 0.7.

Table 2
Level of PMV and PPD [44].

PMV	[−3, −2.5]	[−2.5, −1.5]	[−1.5, −0.5]	[−0.5, +0.5]	[+0.5, +1.5]	[+1.5, +2.5]	[+2.5, +3]
PPD	95–100%	50–95%	10–50%	0–10%	10–50%	50–95%	95–100%
Thermal perception	Cold	Cool	Slightly cool	Neutral (Comfortable)	Slightly warm	Warm	Hot

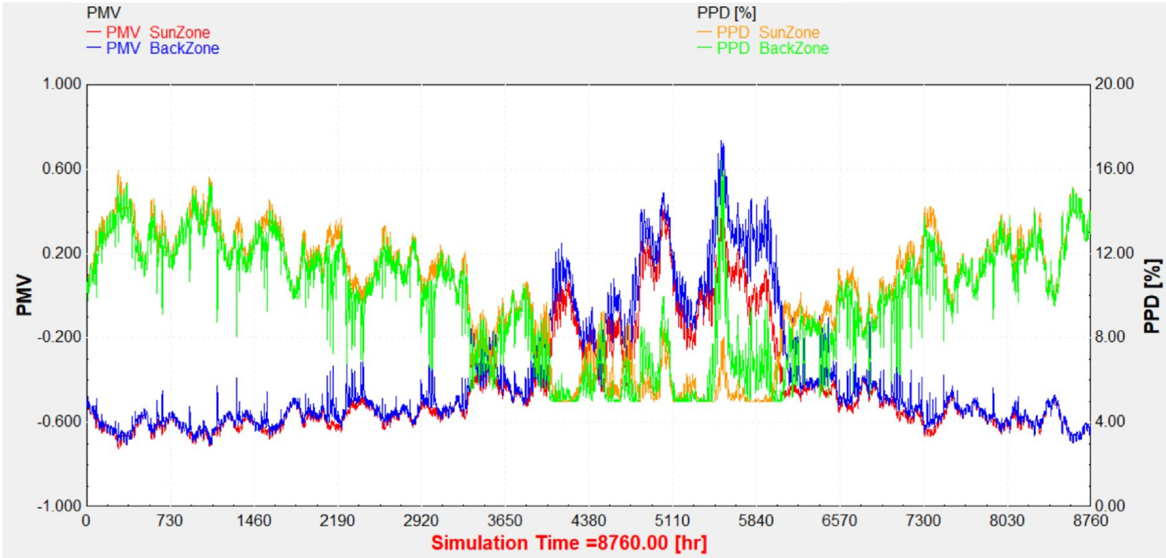

Fig. 12. Variability of PMV and PPD.

Table 3
Energy maximum peak value.

Scenario analysed	Heat demand Sun-Zone W/m^2	Heat demand Back-Zone W/m^2	Cooling demand Sun-Zone W/m^2	Cooling demand Back-Zone W/m^2
2	9.24	8.98	0	13.6
3	5.42	5.09	8.28	18.39
4	8.43	7.90	5.40	15.35
5	19.32	18.74	0	11.39
6	26.75	26.12	0	6.08
7	26.75	26.12	0	6.08

Table 4
Annual heating and cooling demand.

Scenario analysed	Heat demand Sun-Zone W/m^2	Heat demand Back-Zone W/m^2	Cooling demand SunZ-one W/m^2	Cooling demand Back-Zone W/m^2
2	24565.70	14884.11	0	1262.42
3	6713.16	2831.78	6997.02	13128.95
4	13320.83	7405.64	2469.57	6781.20
5	49129.12	37434.65	0	219.73
6	74698.11	61699.71	0	31.20
7	74698.11	61699.71	0	31.20

3. Conclusions

Constantly rising energy prices, and additionally the desire to reduce environmental impact by reducing pollutants emitted into the atmosphere, encourage the search for solutions to optimise building structures and installations while maintaining comfort for users. It is well known that depending on the thermal insulation of the building envelope (and its value of heat transfer coefficient) the amount of energy supplied to the building will vary. In extreme cases it can happen that the internal heat gains may be sufficient to cover all heating needs. However, including infiltration in the calculation indicates that heating of the fresh air supplied from outside is required and significantly affects the total energy demand.

This paper analyses the energy demand of a detached single-family building with an unheated attic. The definition of the building model in TRNSYS software is presented step by step. Then, 7 scenarios of heating and cooling demand in the northern and southern zones were analysed:

1. Building geometry with assigned construction of partitions
2. Scenario 1 + assignment of ideal heating and cooling,
3. Scenario 2 + heat gains from people, lighting, and equipment,
4. Scenario 3 + schedules,
5. Scenario 4 + infiltration 0.6,
6. Scenario 4 + infiltration 1,
7. Scenario 4 + the impact of defining thermal comfort.

The maximum peak value are presented in Table 3. In contrast, the annual heating and cooling demand is presented in Table 4.

The differences in total annual energy demand that occur between the different scenarios confirm how important it is to accurately determine the building's construction and occupancy. This has a huge impact on the choice of energy source for the building. Between the first and last scenario analysed, the difference in total annual energy demand for heating and cooling is 70.16%. The results presented did not take into account the energy needs for hot water preparation, which in a real building should be taken into account when selecting the heat source. In addition, consideration should be given to how to improve thermal comfort so that as few people as possible feel discomfort within the room. Since photovoltaic systems for domestic users are among the most preferred installations further research will focus on the selection of a PV and PV/T systems for the building under consideration. In addition, it will be verified that the selected PV and PV/T installation is capable of making the building energy self-sufficient under London's climatic conditions.

Declaration of competing interest

The authors declare that they have no known competing financial interests or personal relationships that could have appeared to influence the work reported in this paper.

Acknowledgements

The research presented in this paper has received funding from the European Union's Horizon 2020 research and innovation programme Cultural-E under grant agreement N. 870072.

References

[1] Jouhara H, Olabi AG. Editorial: industrial waste heat recovery. Energy 2018;160:1–2. https://doi.org/10.1016/j.energy.2018.07.013.
[2] Malinauskaite J, Jouhara H, Egilegor B, Al-Mansour F, Ahmad L, Pusnik M. Energy efficiency in the industrial sector in the EU, Slovenia, and Spain. Energy 2020;208:118398. https://doi.org/10.1016/j.energy.2020.118398.
[3] Olabi AG, Onumaegbu C, Wilberforce T, Ramadan M, Abdelkareem MA, Al – Alami AH. Critical review of energy storage systems. Energy 2021;214: 118987. https://doi.org/10.1016/j.energy.2020.118987.
[4] Olabi AG, Abdelkareem MA. Renewable energy and climate change. Renew Sustain Energy Rev 2022;158(November 2020):112111. https://doi.org/10.1016/j.rser.2022.112111.
[5] Department for business energy & industrial strategy, "energy trends december 2021 UK, july to september 2021. 2021.
[6] Alami AH, Ramadan M, Abdelkareem MA, Alghawi JJ, Alhattawi NT, Mohamad HA, Olabi AG. Novel and practical photovoltaic applications. Therm Sci Eng Prog 2022;29(July 2021):101208. https://doi.org/10.1016/j.tsep.2022.101208.
[7] Khordehgah N, Żabnieńska-Góra A, Jouhara H. Energy performance analysis of a PV/T system coupled with domestic hot water system. Chem. Eng. 2020;4(2):22. https://doi.org/10.3390/chemengineering4020022.
[8] National Statistics, "Solar photovoltaics deployment (Excel)," Department for Business, Energy & Industrial Strategy, 2022. [Online]. Available: https://www.gov.uk/government/statistics/solar-photovoltaics-deployment. [Accessed: 27-Jan-2022].
[9] Ahmad L, Khordehgah N, Malinauskaite J, Jouhara H. Recent advances and applications of solar photovoltaics and thermal technologies. Energy 2020;207:118254. https://doi.org/10.1016/j.energy.2020.118254.
[10] Official Statistics, "Solar photovoltaic (PV) cost data (Excel)," Department for Business, Energy & Industrial Strategy, 2022. [Online]. Available: https://www.gov.uk/government/statistics/solar-pv-cost-data. [Accessed: 27-Jan-2022].
[11] MCS. The MCS installations Database. 2022. [Online]. Available: https://certificate.microgenerationcertification.org/. [Accessed January 2022].
[12] Laib I, Hamidat A, Haddadi M, Ramzan N, Olabi AG. Study and simulation of the energy performances of a grid-connected PV system supplying a residential house in north of Algeria. Energy 2018;152:445–54. https://doi.org/10.1016/j.energy.2018.03.157.
[13] Maghrabie HM, Abdelkareem MA, Elsaid K, Sayed ET, Radwan A, Rezk H, Wilberforce T, Abo-Khalil AG, Olabi AG. A review of solar chimney for natural ventilation of residential and non-residential buildings. Sustain Energy Technol Assessments 2022;52(PB):102082. https://doi.org/10.1016/j.seta.2022.102082.
[14] Mazzeo D, Matera N, Cornaro C, Oliveti G, Romagnoni P, De Santoli L. EnergyPlus, IDA ICE and TRNSYS predictive simulation accuracy for building thermal behaviour evaluation by using an experimental campaign in solar test boxes with and without a PCM module. Energy Build 2020;212. https://doi.org/10.1016/j.enbuild.2020.109812.
[15] Guarino F, et al. Integration of building simulation and life cycle assessment: a TRNSYS application. Energy Proc 2016;101(September):360–7. https://doi.org/10.1016/j.egypro.2016.11.046.
[16] Nageler P, et al. Validation of dynamic building energy simulation tools based on a real test-box with thermally activated building systems (TABS). Energy Build 2018;168:42–55. https://doi.org/10.1016/j.enbuild.2018.03.025.
[17] Lan B, Tian Z, Niu J, Sun W. Improving the design method of a solar heating system considering weather uncertainty and system reliability. Energy Build 2020;208:109606. https://doi.org/10.1016/j.enbuild.2019.109606.
[18] Magni M, Ochs F, De Vries S, Maccarini A, Sigg F. Detailed cross comparison of building energy simulation tools results using a reference office building as a case study. Energy Build 2021;250:111260. https://doi.org/10.1016/j.enbuild.2021.111260.
[19] Chong A, Gu Y, Jia H. Calibrating building energy simulation models: a review of the basics to guide future work. Energy Build 2021;253:111533. https://doi.org/10.1016/j.enbuild.2021.111533.
[20] Trucano TG, Swiler LP, Igusa T, Oberkampf WL, Pilch M. Calibration, validation, and sensitivity analysis: what ' s what. Reliab Eng Syst Saf 2006;91:1331–57. https://doi.org/10.1016/j.ress.2005.11.031.
[21] Khordehgah N, Guichet V, Lester SP, Jouhara H. Computational study and experimental validation of a solar photovoltaics and thermal technology. Renew Energy 2019;143:1348–56. https://doi.org/10.1016/j.renene.2019.05.108.
[22] Yu Y, Yang H, Peng J, Long E. Performance comparisons of two flat-plate photovoltaic thermal collectors with different channel configurations. Energy 2019;175:300–8. https://doi.org/10.1016/j.energy.2019.03.054.
[23] Brough D, Ramos J, Delpech B, Jouhara H. Development and validation of a TRNSYS type to simulate heat pipe heat exchangers in transient applications of waste heat recovery. Int. J. Thermofluids 2021;9. https://doi.org/10.1016/j.ijft.2020.100056.
[24] Venturelli M, Brough D, Milani M, Montorsi L, Jouhara H. Comprehensive numerical model for the analysis of potential heat recovery solutions in a ceramic industry. Int. J. Thermofluids 2021;10:100080. https://doi.org/10.1016/j.ijft.2021.100080.
[25] Hengel F, Heschl C, Inschlag F, Klanatsky P. System efficiency of pvt collector-driven heat pumps. Int. J. Thermofluids 2020;5(6):100034. https://doi.org/10.1016/j.ijft.2020.100034.
[26] Lee M, Lee D, Park MH, Kang YT, Kim Y. Performance improvement of solar-assisted ground-source heat pumps with parallelly connected heat sources in heating-dominated areas. Energy 2022;240:122807. https://doi.org/10.1016/j.energy.2021.122807.
[27] Calise F, Cappiello F, D'Agostino D, Vicidomini M. Heat metering for residential buildings: a novel approach through dynamic simulations for the calculation of energy and economic savings. Energy 2021;234:121204. https://doi.org/10.1016/j.energy.2021.121204.
[28] G. Battista, E. de Lieto Vollaro, P. Ocłoń, and A. Vallati, "Effect of mutual radiative exchange between the surfaces of a street canyon on the building thermal energy demand," Energy, vol. 226, 2021, doi: 10.1016/j.energy.2021.120346.
[29] Korpela T, et al. Waste heat recovery potential in residential apartment buildings in Finland's Kymenlaakso region by using mechanical exhaust air ventilation and heat pumps. Int. J. Thermofluids 2022;13:100127. https://doi.org/10.1016/j.ijft.2021.100127. November 2021.
[30] Lipinski T, Ahmad D, Serey N, Jouhara H. Review of ventilation strategies to reduce the risk of disease transmission in high occupancy buildings. Int. J. Thermofluids 2020;7(8):100045. https://doi.org/10.1016/j.ijft.2020.100045.
[31] Rashad M, Khordehgah N, Żabnieńska-Góra A, Ahmad L, Jouhara H. The utilisation of useful ambient energy in residential dwellings to improve thermal comfort and reduce energy consumption. Int. J. Thermofluids 2021;9. https://doi.org/10.1016/j.ijft.2020.100059.
[32] Suite of Tools." [Online]. Available: http://www.trnsys.com/features/suite-of-tools.php.html. [Accessed February 2022].
[33] Feng Y, Yao J, Li Z, Zheng R. Uncertainty prediction of energy consumption in buildings under stochastic shading adjustment. Energy 2022;254:124145. https://doi.org/10.2139/ssrn.3983066.
[34] Chegari B, Tabaa M, Simeu E, Moutaouakkil F, Medromi H. An optimal surrogate-model-based approach to support comfortable and nearly zero energy buildings design. Energy 2022;248:123584. https://doi.org/10.1016/j.energy.2022.123584.
[35] Huang B, Wang Y, Lu W, Cheng M. Fabrication and energy efficiency of translucent concrete panel for building envelope. Energy 2022;248:123635. https://doi.org/10.1016/j.energy.2022.123635.
[36] Office for National Statistic. Energy efficiency of housing in England and wales: 2021. 2021. [Online]. Available: https://www.ons.gov.uk/peoplepopulationandcommunity/housing/articles/energyefficiencyofhousinginenglandandwales/2021. [Accessed January 2022].
[37] Hm Government. The building Regulations 2010, conservation of fuel and power L1 A, Volume 1: dwellings, 2021 edition – for use in England, vol. 1; 2021.
[38] International Organization for Standardization. ISO 6946:2017 – building components and building elements - thermal resistance and thermal transmittance. 2017. Switzerland.
[39] Klein MJDSA, Beckman WA, Mitchell JW, Duffie JA, Duffie NA, Freeman TL, Mitchell JC, Braun JE, Evans BL, Kummer JP, Urban RE, Fiksel A, Thornton JW, Blair NJ, Williams PM, Bradley DE, McDowell TP, Kummert M, Arias DA. Trnsys 17 2009;5:1–29.
[40] CIBSTE. Guide B1: heating. 2016.

[41] Song B, Bai L, Yang L. Analysis of the long-term effects of solar radiation on the indoor thermal comfort in office buildings. Energy 2022;247:123499. https://doi.org/10.1016/j.energy.2022.123499.
[42] Pourshaghaghy A, Omidvari M. Examination of thermal comfort in a hospital using PMV-PPD model. Appl Ergon 2012;43(6):1089–95. https://doi.org/10.1016/j.apergo.2012.03.010.
[43] ISO, ISO 7730:2005. Ergonomics of the thermal environment — analytical determination and interpretation of thermal comfort using calculation of the PMV and PPD indices and local thermal comfort criteria. 2005.
[44] Dong Z, Boyi Q, Pengfei L, Zhoujian A. Comprehensive evaluation and optimization of rural space heating modes in cold areas based on PMV-PPD. Energy Build 2021;246:111120. https://doi.org/10.1016/j.enbuild.2021.111120.